Bull Volcanol (1991) 53:533–545

Bulletin of
Volcanology

Real-time Seismic Amplitude Measurement (RSAM): a volcano monitoring and prediction tool

Elliot T Endo[1] **and Tom Murray**[2]

[1] U.S. Geological Survey, APO New York, NY 09697-7002, USA
[2] Cascades Volcano Observatory, 5400 MacArthur Blvd., Vancouver, WA 98661, USA

Received April 20, 1990/Accepted February 2, 1991

Abstract. Seismicity is one of the most commonly monitored phenomena used to determine the state of a volcano and for the prediction of volcanic eruptions. Although several real-time earthquake-detection and data acquisition systems exist, few continuously measure seismic amplitude in circumstances where individual events are difficult to recognize or where volcanic tremor is prevalent. Analog seismic records provide a quick visual overview of activity; however, continuous rapid quantitative analysis to define the intensity of seismic activity for the purpose of predicting volcanic eruptions is not always possible because of clipping that results from the limited dynamic range of analog recorders. At the Cascades Volcano Observatory, an inexpensive 8-bit analog-to-digital system controlled by a laptop computer is used to provide 1-min average-amplitude information from eight telemetered seismic stations. The absolute voltage level for each station is digitized, averaged, and appended in near real-time to a data file on a multiuser computer system. Raw real-time seismic amplitude measurement (RSAM) data or transformed RSAM data are then plotted on a common time base with other available volcano-monitoring information such as tilt. Changes in earthquake activity associated with dome-building episodes, weather, and instrumental difficulties are recognized as distinct patterns in the RSAM data set. RSAM data for dome-building episodes gradually develop into exponential increases that terminate just before the time of magma extrusion. Mount St. Helens crater earthquakes show up as isolated spikes on amplitude plots for crater seismic stations but seldom for more distant stations. Weather-related noise shows up as low-level, long-term disturbances on all seismic stations, regardless of distance from the volcano. Implemented in mid-1985, the RSAM system has proved valuable in providing up-to-date information on seismic activity for three Mount St. Helens eruptive episodes from 1985 to 1986 (May 1985, May 1986, and October 1986). Tiltmeter data, the only other telemetered geophysical information that was available for the three dome-building episodes, is compared to RSAM data to show that the increase in RSAM data was related to the transport of magma to the surface. Thus, if tiltmeter data is not available, RSAM data can be used to predict future magmatic eruptions at Mount St. Helens. We also recognize the limitations of RSAM data. Two examples of RSAM data associated with phreatic or shallow phreatomagmatic explosions were not preceded by the same increases in RSAM data or changes in tilt associated with the three dome-building eruptions.

Offprint requests to: E T Endo

Introduction

Premonitory earthquake activity is a key indicator of the state of a volcano and the potential for volcanic eruptions (Decker 1973, 1986; Malone et al. 1983; Minakami 1960, 1974; Minakami et al. 1969; Swanson et al. 1985). Provided discrete earthquakes can be recognized, the type and intensity of seismic activity is often expressed by the number of earthquakes per unit time, by earthquake magnitude, seismic-energy release, b-value, or as earthquake source parameters for the purpose of predicting volcanic eruptions.

For Mount St. Helens the Cascades Volcano Observatory (CVO) relies on the Geophysics Program, University of Washington for routine earthquake information such as hypocenter locations, magnitudes, and focal mechanism solutions to determine the state of the volcano. Although highly desirable, access to near real-time (within a few minutes) seismic information was not available prior to 1985. An earthquake count of CVO analog seismic records that were changed every 3 h provided the most up-to-date information on seismic activity. Manual counts were appended to a file on a multiuser computer, where data could be compared with other volcano-monitoring measurements such as tilt, sulphur dioxide output, total magnetic field, and EDM (*e*lectronic *d*istance *m*easurement) line changes. Such an earthquake count provided only minimal in-

formation on the current state of seismic activity because it was at least several hours out of date at all times. While the cumulative earthquake count for any swarm associated with an eruption is an approximate measure of intensity (proportional to total seismic energy provided earthquakes are similar in magnitude) of earthquake activity, the count is subject to inconsistencies of analog seismic record interpretation, questionable gain changes, and loss of data due to overlapping traces, clipped seismic signals, missed record changes or telemetry failure. Thus, earthquake counts prior to and during an eruption are not always quantitatively reliable.

Premonitory seismicity associated with several Mount St. Helens eruptive episodes during 1984 was characterized by intense earthquake swarms that began with discrete earthquakes recorded on seismic stations located less than 1.5 km from the center of the dome, then progressed to continuous high-amplitude signals. The intense seismicity associated with the eruptive episode of 10 September 1984 was a motivating factor in implementation of a real-time seismic amplitude measurement system. In less than 24 h seismicity progressed from discrete events (Fig. 1a) to an almost continuous succession of earthquakes that could not be counted individually (Fig. 1b). The inability to count earthquakes and to measure coda lengths resulted in an inaccurate estimate of seismic energy released before the eruption. One method used to reduce inaccuracies was to rely on more distant seismic stations not affected by the increase in smaller magnitude earthquakes. However a potential problem with using another seismic record for earthquake counts and coda measurements was the bias toward counting only larger magnitude events and introducing a systematic error in seismic energy estimates utilizing coda-magnitudes. What was needed was a monitoring technique that was capable of providing an easy-to-access and plot continuous time history of relative seismic intensity related to eruptions.

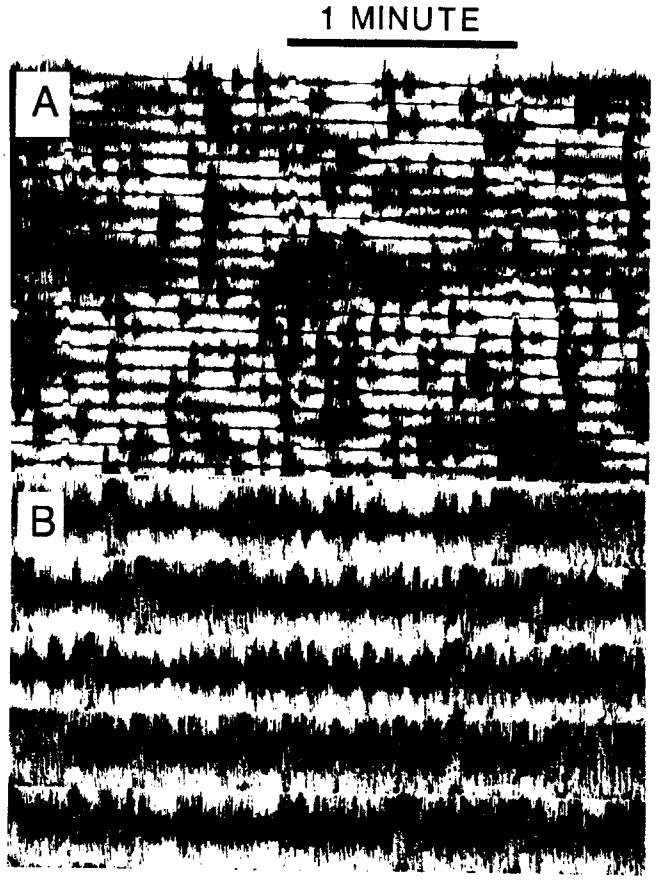

Fig. 1. A A section of 8 September 1984 analog seismic record for the seismic station GDN located 700 m N of the geometric center of the lava dome. Lines are spaced 15 min apart and the section is about 3 min wide. **B** A section of 9 September 1984 analog seismic record for GDN showing the intense seismic activity that preceded the 10 September 1984 dome-building eruption

This paper describes a real-time seismic amplitude measurement or RSAM system that provides the continuous high-resolution real-time measurements that met our requirement to produce easily repeated measurements of relative seismic intensity from one volcanic event to the next. Furthermore, in digital form the data are easy to plot with the aid of a computer and compare with other real-time data, such as tilt or geochemical-monitoring data. The amplitude measurements accurately define the relative intensities of eruptive episodes regardless of the type of seismic activity (discrete earthquakes, closely spaced earthquakes, volcanic tremor, or mudflows). However, the present system does not provide spectral information like the system described by Hurst (1985) or Nishi (1987). For event discrimination, the lack of spectral information with RSAM data is a limiting factor in identification (without an analog seismic record) of volcanic tremor, fumarolic noise, wind noise, or noise generated by other sources.

The idea of monitoring the mean amplitudes of seismic records is not new. Sassa (1936) utilized daily mean amplitudes to describe the state of volcano Aso in Japan more than 50 years ago. Nakamura (1977) briefly described a similar technique for measuring acoustic emissions associated with fracturing using an RMS (root-mean square) voltmeter. Although the initial application of the RSAM system did not consider monitoring of harmonic or volcanic tremor, RSAM is ideally suited for continuous measurement of mean amplitude as suggested by Schick et al. (1982) and Schick (1988) to document the seismic time history associated with volcanic eruptions. Schick obtained an analog recording of the mean envelope amplitude by feeding the demodulated output from a magnetic tape recording to a bridge rectifier and a low pass filter. Whatever the technique used to measure seismic amplitudes, it is important to understand how the measurements are related to the process being monitored.

To clearly show that RSAM data can be used for monitoring and predicting dome-building episodes at Mount St. Helens, we compare RSAM data with telemetered tiltmeter data to show changes in RSAM data are related to the migration of magma from shallow depth to the surface of the earth. Because of the importance of tiltmeter data to our interpretation of RSAM

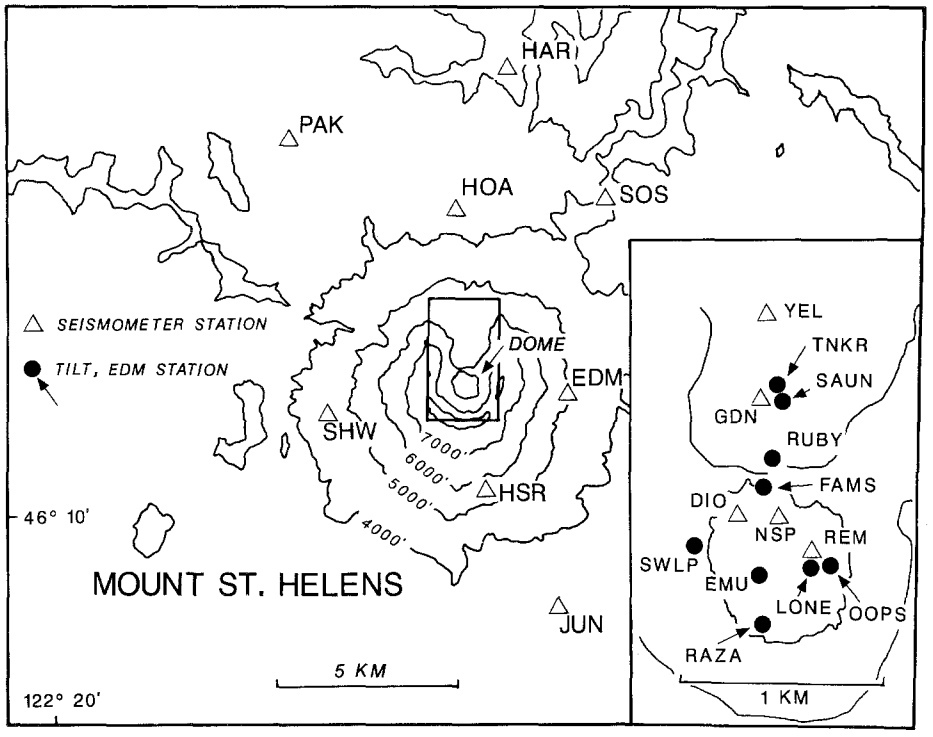

Fig. 2. The physiography of Mount St. Helens, Washington, and locations of seismic stations (*open triangles*) and telemetered tiltmeter sites (*closed circles*). Seismic station ERT, located 16 km to the W, has not been plotted. *SHW, SOS, JUN, HSR,* and *EDM* are maintained by the University of Washington. All other seismometer stations and tilt meter sites are maintained by CVO. Tiltmeter stations *EMU, TNKR,* and *RUBY,* were operational in May of 1985. *SAUN* and *RUBY* were operating in May 1986. *FAMS, OOPS, RAZA,* and *SWLP* were operating in October 1986. *LONE* is the current location of a gas sensor and displacement meter. The Mount St. Helens lave dome is indicated by the *2000 m topographic contour*

data, we give a detailed description of tiltmeter instrumentation and tiltmeter data. Two examples of RSAM data associated with shallow explosions are included in this paper to point out the limitation of RSAM data in predicting phreatic or phreatomagmatic explosions.

Seismic network and instrumentation

Seismic information at the Cascades Volcano Observatory is provided by analog signals from three stations located in the 1980 crater, station NSP (destroyed in April 1986, replaced by DIO in September 1986 and later by REM in January 1987), GDN, and YEL (Fig. 2). Five additional stations that provide information (HOA, SHW, EDM, PAK, and ERT) are located outside the crater at distances of as much as 16 km from the vent. Six stations are maintained by the Cascades Volcano Observatory and the remainder are maintained by the University of Washington.

Each seismic station consists of a 1-Hz vertical seismometer, a preamp/voltage-controlled oscillator, and a low-output-power VHF or UHF radio frequency transmitter (100–150 milliwatts). External resistance for each seismometer station was adjusted for 0.7–0.8 critical damping. Typical loaded-motor constants are approximately 1.0 V/cm/s. The total response of the system is similar to that used by the US Geological Survey in California (Lee and Stewart 1981) and Hawaii (Koyanagi et al. 1975). The 3-db points for the system electronics are 0.1 Hz and 25 Hz. The displacement response peaks at 15 Hz. Frequency-multiplexed seismic-carrier signals are transmitted from Mount St. Helens to CVO in Vancouver, Washington (>75 km) via several radio repeater links.

At CVO, audio carrier outputs from radio receivers are demodulated by a bank of discriminators. Discriminator outputs were adjusted for a maximum of ±2.5 volts output for ±125 Hz deviation of carrier signals. Discriminator outputs are fed to an absolute value circuit that in turn is interfaced with the 8-bit analog-to-digital (A/D) system described below. Unlike recorders, where pen driver gains are easily adjusted by a switch, inputs to the A/D converter are fixed and cannot be adjusted without an electronic circuit modification of either the discriminator or the input-signal conditioning of the A/D converter, thus preventing undocumented changes in recording sensitivity.

RSAM instrumentation, data acquisition, analysis, and interpretation

RSAM instrumentation

The real-time seismic-amplitude measurement system consists of a Tandy (Radio Shack) model 100 laptop computer, an Elexor data-acquisition unit, and an in-house designed signal conditioner/multiplexor board (Fig. 3). Mounting the in-house board inside the Elexor unit keeps the total size of the analyzer to a minimum (32 × 24 × 12 cm). The model 100 and the Elexor units are designed to run on either internal or external batteries. With a total current draw of less than 100 ma at 12 V, the entire unit can be powered easily by a single 12 V car battery. The signal conditioner/multiplexor buffers the eight seismic signals, removes any dc components, and amplifies the signals to take full advantage of the range (0–5 V) of the analog-to-digital converter (A/D). A CMOS (complementary metal oxide

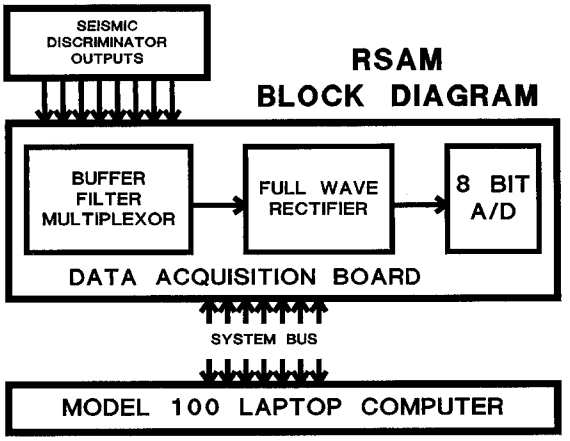

Fig. 3. Block diagram of RSAM system from the analog inputs to laptop computer system

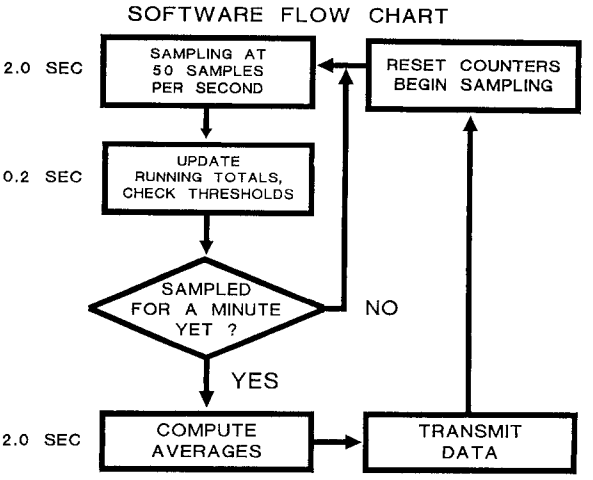

Fig. 4. Flow chart indicating software actions in the data acquisition process and the preprocessing of data prior to transmission to a minicomputer

semi-conductor) multiplexor selects the desired seismic signal for digitizing. The negative component of the signal is converted to a positive voltage by a full-wave rectifier before it is digitized by the 8-bit A/D. Control of the multiplexor and acquisition of the data are accomplished by using the model 100's system bus, freeing the computer's printer, modem, cassette, and RS-232C ports for connection to other peripherals. An 8-bit digital-output port of the Elexor unit controls the eight LEDs and buzzer for the threshold alarms.

RSAM data acquisition and analysis

The model 100 computes the average absolute signal amplitude once per minute for each input channel by dividing the sum of each channel's digitized samples by the number of samples. Taking an average once per minute allows the cessation of data acquisition for short periods in order to process the data. This greatly simplifies programming because data acquisition and processing do not have to be performed concurrently. The analyzer's software can be divided into four programs: data acquisition, threshold detection, average computation, and data transmission. The speed necessary to sample eight channels at 50 times per second required the data acquisition program to be written in machine code. The resident language (BASIC) is used in the other programs where speed is not a requirement. These programs take about 7 s/min., leaving the other 53 s/min. for data acquisition (Fig. 4). When the data acquisition program is called from BASIC, it collects data for 2 s (50 samples/channel) and returns the sum of the samples for each channel. Because it is written in machine code, it is very efficient and takes only about 1 ms to get one sample for each of the 8 channels. At 50 samples per s, 95% of the sampling time is spent waiting to take the next group of samples. This time is available for additional processing.

The sums returned by the data-acquisition program are checked against thresholds set by the user. If any of the thresholds are exceeded, a buzzer is activated and LEDs corresponding to the station or stations that have exceeded their thresholds are lit. They remain lit and the buzzer continues to sound until the sums fall below their thresholds. A running total of the returned sums for each channel is kept throughout each minute. At the end of the minute, these running total are divided by the number of samples taken in the minute. The resulting averages and the time are transmitted to the minicomputer via the RS-232C port of the model 100. The running totals and the number of samples are reset to zero and data acquisition for the next minute is resumed. When 1-min averages have been computed and sent to the minicomputer, stored data have been converted from counts which have a maximum of 255 for the 8-bit A/D system, to average volts. Digital counts were multiplied by 10 to allow plotting at an optimal scale. Discriminator outputs are ± 2.5 volts peak-to-peak, but only absolute values are recorded. The maximum voltage range of 0 to 2.5 volts for discriminator output and a 0 to 5 volts input range for the A/D, result in a measurement resolution of about 20 mv, or one half the typical peak-to-peak background noise level for each seismic station. Figure 5 shows a block diagram of the current configuration of the telemetered volcano-monitoring system at CVO. Network receivers, the real-time seismic amplitude monitor, and the minicomputer are located at the observatory in Vancouver, Washington. The minicomputer functions as the primary data storage device and also provides a multiuser environment for real-time data analysis of all telemetered data.

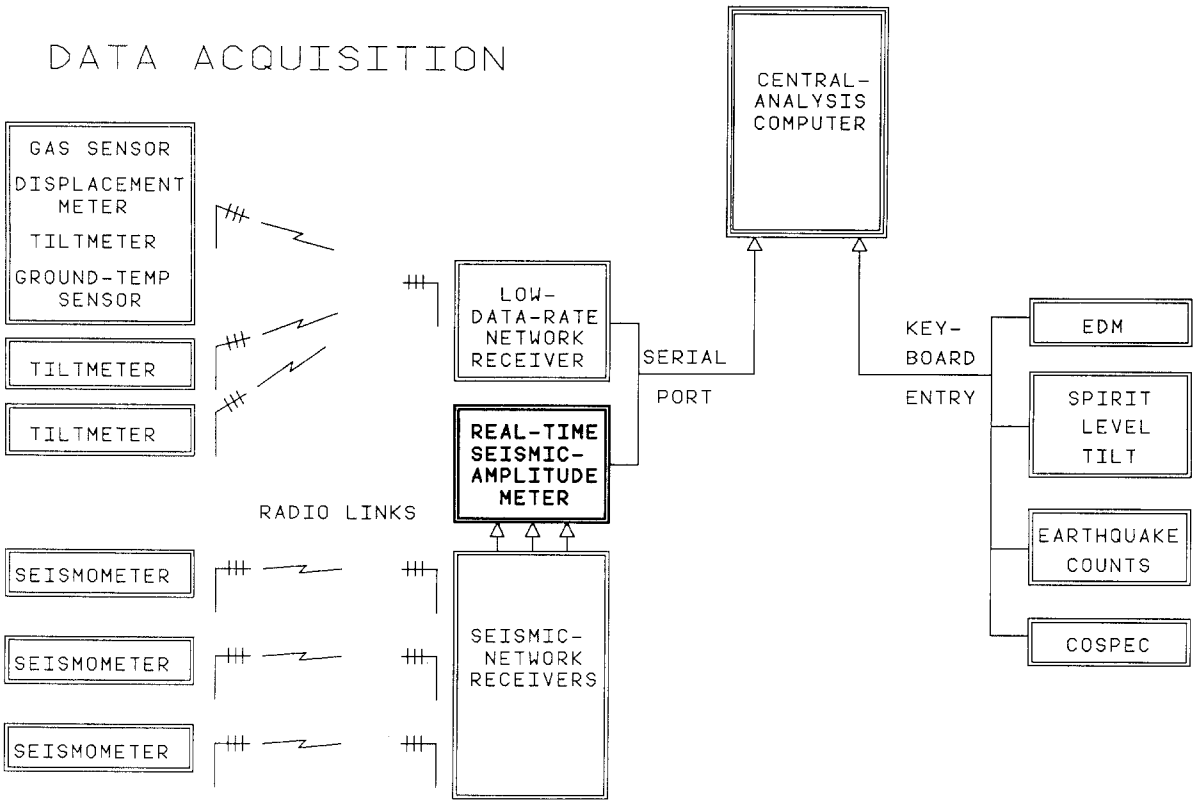

Fig. 5. Block diagram of Mount St. Helens telemetry monitoring system operated by CVO. The keyboard entry of monitoring data into a common data base is no longer done on a routine basis

RSAM data interpretation

Each seismic station uses a velocity transducer (seismometer) with a free period of 1 Hz; thus the measured output is proportional to velocity or V/cm/s for frequencies above 1 Hz. If the absolute response of each transducer were known, then each 1-min average would represent the average ground velocity detected by the seismometer at that seismic station for that minute.

The average ground velocity of seismic waves has no simple relationship to commonly measured earthquake parameters such as magnitude, seismic energy, and seismic moment. At this time, we do not know the precise relationship of electrical energy to seismic energy as defined by Gutenberg and Richter (1956) or Richter (1958), or how it is related to seismic moment (Aki and Richards 1980). However, the output voltage of the discriminator is an easily understood quantity that can be accurately measured. The square of the measured voltage is proportional to electrical power (Korneff 1966). It is a simple measurement that can be repeated, provided there are no significant changes of instrumentation. The physical significance of this power is that it is proportional to the electrical power generated by the geophone responding to the shaking of the Earth at the seismometer site. Total electrical energy is obtained by integrating measured power over time.

The relative changes in seismic wave amplitude (average ground velocity) with distance may give an indication of average depth changes for earthquake sources (Norwack and Aki 1984). A formal approach is to look at the statistical change in the average-amplitude ratios of stations located at different distances from the conduit system (amplitude ratios for a number of stations and perhaps the average ratio over time). A 2-d gaussian beam synthetic model (Norwack and Aki 1984) for Mount St. Helens predicts a significant increase in amplitude ratio for earthquakes that occur at a 1.0-km depth compared to earthquakes that occur at a 3.5-km depth. For earthquakes that cannot be located accurately, alternate interpretations of increasing seismic amplitude are: (1) the source was getting closer to the seismic station in a horizontal plane and (2) there was an increase in the magnitude of earthquakes from a fixed source. At Mount St. Helens, eruption-related earthquake sources are mostly confined to a region close to a small magma chamber and a narrow conduit system (Scandone and Malone 1985). Thus the source of seismic energy prior to eruptions is approximately fixed in space horizontally. For more distant seismic stations, small changes in vertical position are of little consequence.

The seismic data collected from 1985 to 1986 for three dome-building episodes showed similar exponential increases in RSAM data. Rapid changes in telemetered continuous tiltmeter measurements indicated that significant deformation of the dome and (or) nearby crater floor coincided with the rapid increases in seismic activity in the 24–48 h preceding extrusion. By contrast to the nearly identical increases in RSAM data just

prior to the extrusion, RSAM data for the surface phase of dome-building extrusions vary considerably for the three examples presented. Two dome-building eruptions were accompanied by thrust faulting of the crater floor and one resulted in large rockfalls and avalanches from the lava dome. Avalanches and rockfalls associated with individual eruptions depended on the morphology of the dome (where extrusion occurred) and the volume of extrusion. Unlike earthquakes, seismic signals generated by avalanches and rockfalls were usually not recorded at stations located more than 10 km from the event.

Plots of RSAM data provide additional details of the time history of eruptive episodes previously not detected in routine earthquake counts at station YEL. Energy plots of earthquakes and surface events suggested that an eruptive cycle has two possible phases (Malone et al. 1983). The first phase was thought to be associated with increasing stress in country rock due to the movement of magma toward the surface. The second phase consisted of surface events associated with disruption of the dome (avalanches, rockfalls) and the growth of a new lobe on the dome. Although useful inferences can be drawn from seismic data and its relationship to processes, seismicity itself does not necessarily indicate mass transfer from depth to the surface. Surface deformation, such as changes in EDM lines and tilt provided stronger evidence for the effects of magma movement.

Tiltmeter instrumentation and data

Electronic tiltmeters provide a convenient method to measure surface deformation associated with the extrusion of magma. For this paper, electronic tiltmeters have provided data to support interpretation of RSAM data. Several types of platform tiltmeters were used at field sites in the 1980 crater. In most cases, single-axis tiltmeters were used to detect tilt radial to the center of the dome. A few installations had dual-axis tiltmeters that were oriented to detect radial and tangential tilt. Current practice at Mount St. Helens is to install tiltmeters on the dome or within 1 km of the center of the dome. The proximity of tiltmeters to the point of extrusion commonly yields tilts in excess of 10000 microradians. These large tilts reduce concern over diurnal effects, such as those caused by temperature changes, which preculde early detection of much smaller tilts (less than a few microradians) associated with early pre-eruption deformation. Sites on the dome have inclinometers to measure tilt beyond the range of tiltmeters. A typical installation includes a single-axis tiltmeter with a 5 microradian sensitivity and 5000 microradian dynamic range, and an inclinometer with a 300 microradian sensitivity and 30000 microradian dynamic range.

A negative aspect of dome installations is the frequent loss of tiltmeters to the effects of eruptions. Debris from small explosions prior to or accompanying eruptions have damaged or destroyed equipment. Other sites have been lost to rockfalls or avalanches resulting from deformation of the dome. Still others have been buried by newly extruded lava lobes. Figure 2 shows the locations of tiltmeters in operation during the three eruptive episodes monitored by the RSAM system.

Tiltmeter data are telemetered to the Cascades Volcano Observatory via a USGS low-data-rate telemetry system. At programmed intervals (usually 10 min), 13-bit temperature and tilt data from each site are telemetered in digital format. Digital information collected by a set of laptop computers is appended to a file on a multiuser minicomputer. Like RSAM data, tilt data are available on the multiuser minicomputer for routine plotting with other volcano-monitoring data on a common time base.

Since mid-1981, there have been 12 extrusive episodes at Mount St. Helens during which tiltmeters have been in operation. Early installations were intended to determine the best locations to monitor tilt changes. During the eruptive episodes described in this paper, outward tilt of the flanks of the dome accelerated in the last 24 to 48 h prior to extrusion. During 1981–1983, real-time plotting of telemetered tilt data was possible with some difficulty using a minicomputer dedicated to logging the tilt data. In mid-1984, repeated hardware failures spurred the writing and implementation of software to write tilt data directly to files on the CVO VAX 11/750 computer system.

In 1985 a program called BOB (Murray and Endo 1986) was written to plot equally spaced time-series data utilizing more efficient direct-file access available on the VAX computer system. Plot parameters for multiple-frame plots can be easily changed interactively. Since 1985, it has been relatively easy to plot various geophysical data on a common time axis using BOB and a plot-command file. The VAX computer system is also accessible via dial-in ports or any one of the many terminals linked to the computer system.

Real-time Seismic Amplitude Measurement for three dome-building eruptions at Mount St. Helens and comparison to tilt measurements

The May–June 1985 eruptive episode

Narrative. From February 1985 to spring 1987, the RSAM system recorded three dome-building episodes at Mount St. Helens. The first, which occurred in late May 1985, caused substantial disruption of the dome due to endogenous dome growth. A 250×500 m graben oriented east-west formed in the south summit area of the dome accompanied by intense crater floor deformation (thrust faulting, transverse fractures, etc.) of the south crater floor. Although the total volume of intruded and extruded magma was about to 7×10^6 m^3, less than 1×10^6 m^3 was extruded. Formation of the graben structure and associated crater floor deformation accounted for an extended period of seismicity (more than one week) following the initial phase of intense earthquake activity.

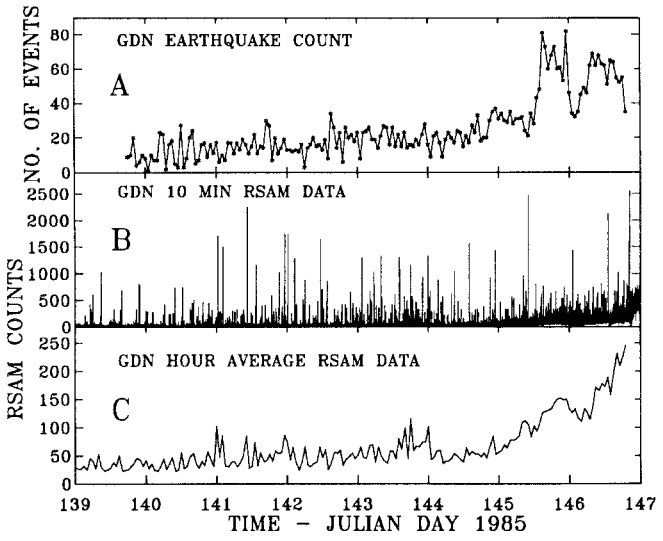

Fig. 6. **A** Plot of hourly earthquake counts from station GDN analog seismic records from 19 May (Julian day 139) to 27 May (Julian day 147), 1985. **B** Plot of 10-min RSAM data for station GDN or raw data for the same time period as **A**. Maximum possible value is 2550 counts. **C** Plot of the hourly average of 1-min RSAM data during the same time period as Fig. 6a and b

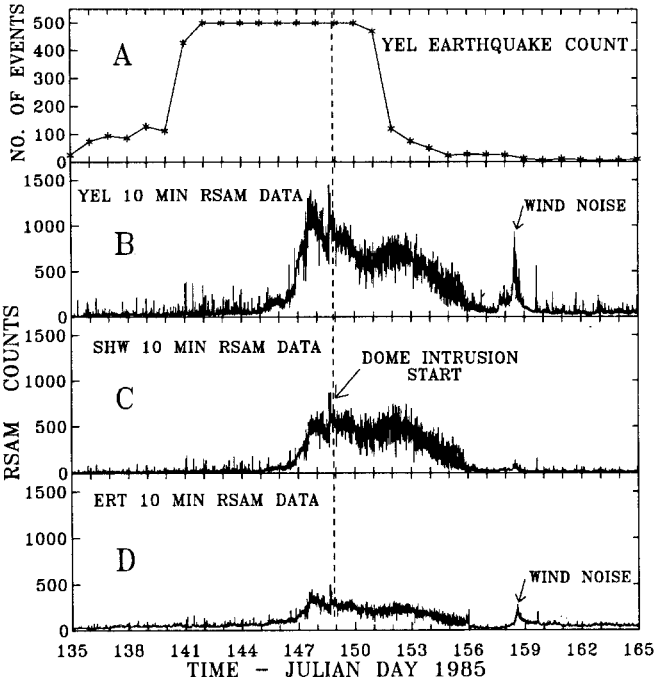

Fig. 7. **A** Plot of manual daily counts for seismic events recognized as earthquakes on station YEL analog seismogram from 15 May (Julian day 135) to 14 June (Julian day 165), 1985. **B** Plot of 10-min RSAM data for station YEL from 15 May (Julian day 135) to 14 June (Julian day 165), 1985. **C** Plot of 10-min RSAM data for station SHW. Although SHW is located about 3× the YEL distance from the dome, the SHW 10-min plot mimics the YEL 10-min plot. **D** The bottom frame is a plot of 10-min RSAM data for the ERT seismic station. Like SHW, ERT 10-min average mimics RSAM plot for station YEL at a lower amplitude. The period from 25 May (Julian day 145) to about 0000 UT 28 May (Julian day 148, 1700 PDT) was the period of intense seismicity associated with the magma-migration phase of the May 1985 eruption. The period from 0000 UT 28 May (Julian day 148) to 5–6 June (Julian days 156–157), and labeled dome intrusion was a period of extended seismic activity thought to be associated with the dome's graben formation

RSAM data. During mid-May 1985, crater seismic stations GND and YEL showed an increase in the total number of earthquakes recorded daily. On 16 May (Julian day 136), the earthquake count for seismic station YEL exceeded ten events per day compared to less than one event per day during March–April. By 1800 UT 19 May (Julian day 139), the count at station GDN was as much as 9–10 events per hour (Fig. 6a). Criteria for an event that was counted consisted of a minimum peak-to-peak amplitude of 8 mm and-or a minimum coda duration of 10 s. GDN is located about 700 m north of the geometric center of the dome. Figure 6b and c illustrate just two of several types of plots possible with RSAM data. Each average value for 10 min is plotted as a bar in the middle frame. In the lower frame, 1-h average RSAM data was plotted as a line graph. During 19–25 May (Julian days 139–145), the hourly event count from the RSAM data mimicked the manual hourly count of the seismogram for station GDN. Hourly earthquake counts were made on seismograms with a rotation rate of 120–240 mm/min and a translation rate of 8 mm per revolution. The decrease shown in the manual earthquake counts at GDN seismic station does not show up as strongly in the RSAM count because of the increasing maximum amplitudes of individual earthquakes. Inclement weather prevented field observations of the start of extrusion, which occurred between 27 May and 29 May (Julian days 147 and 149).

Figure 7 illustrates the advantage of using RSAM data instead of manual earthquake counts during periods of intense earthquake activity. Daily counts were made on seismograms with a rotation rate of 60 mm/min and translation rate of 2.5 mm each 15 min. Due to the rotation rate and the translation rate, and the near clipping amplitudes, the maximum number of individual earthquakes that could be identified on the seismograms was about 500 per day (Fig. 7a). YEL is located about 1200 m north of the geometric center of the dome. While overlapping seismic signatures limited the maximum daily earthquake count to about 500 events, RSAM data continued to provide meaningful information on seismic activity throughout the eruptive episode. Plots of 10-min RSAM data for the period bracketing the eruption are shown in Figs. 7b–d. Data are from seismic stations YEL, SHW, and ERT. Although these stations are spaced almost 16 km apart, the plot for the most distant station (ERT) mimics the plot for the nearest station (YEL). On 7 June 1985 (Julian days 158–159), a strong weather front moved through the area and produced increased average amplitudes at all seismic stations.

Tilt data. The May 1985 eruptive episode was the first to be recorded by the RSAM system. There were three tiltmeters (Fig. 2) operating at the time on or near the

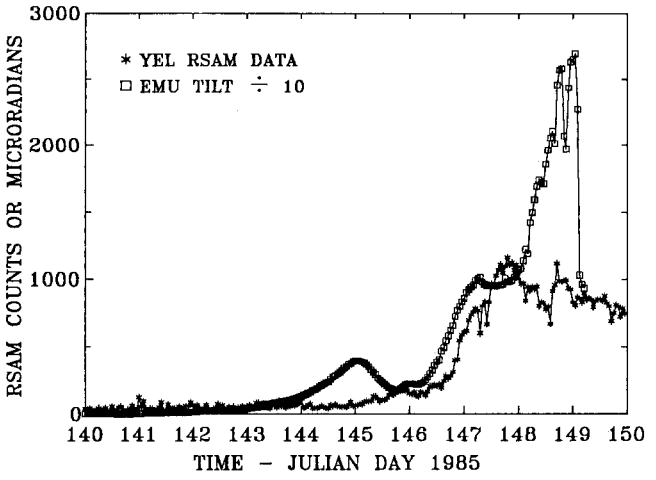

Fig. 8. Hourly average RSAM digital counts for seismic station YEL and tilt for EMU tiltmeter station for the May 1985 dome-building eruption plotted on a common horizontal scale. Tilt data scaled for plotting adjacent to the RSAM curve

dome. Both RUBY, on the north flank of the dome, and EMU, in the south summit area of the dome, showed rapid increase in tilt at the same time as the RSAM data increased in absolute average amplitude. Figure 8 shows tilt at the EMU site and RSAM data from seismic station YEL plotted on the same time scale. The tiltmeter at the TNKR site, located on the crater floor about 750 m north of the center of the dome, was unreliable during this period. During 26–27 May (Julian days 146–147), both YEL RSAM data and EMU tilt measurements showed rapid increases in data values that we assume were associated with the rapid migration of magma up the conduit system. By 28 May (Julian day 148), EMU showed additional rapid tilt associated with the development of the graben. Early on 29 May (Julian day 149), telemetry from the EMU site terminated due to intense disruption of the ground around the station. The net tilt at EMU as about 33 000 microradians, north down.

The May 1986 eruptive episode

Narrative. The early May 1986 eruptive episode produced a dacite lobe about 250 m wide and 500 m long near the center of the dome. The estimated volume of intruded and extruded material is about 9×10^6 m^3. The episode was preceded by a month of almost daily small explosion events. One explosion event (accompanied by discharge of gas, ash, and other vent debris; see cover photo of Science, vol. 221, no. 4618 for the photograph of an example) on 16 April (Julian day 106) disabled the first radio-telemetered seismic station NSP on the dome. A subsequent explosion on 19 April (Julian day 109) tossed lava blocks more than 1 km north of the dome and was accompanied by three small debris flows from the dome; resulting hot rocks were dislodged from the dome by the explosion. As in the May 1985 episode, the exact time of extrusion could not be determined by field observation. The period of intense seismicity thought to be associated with rapid magma migration lasted less than 24 h (Endo et al. 1987). Within 24 h this was followed by a period of rockfall-avalanche activity from the growing lobe of lava.

RSAM data. Although the eruption of May 1986 was preceded by almost a month of small explosions and other precursor seismic activity, much of the migration of magma from a depth of 2–3 km to the surface took place in the last 24 h before extrusion began (Endo et al. 1987). Earthquake counts for seismic station YEL exceeded 10 per day starting on 25 April (Julian day 115). Seismic station SHW showed a significant increase in seismicity on 30 April (Julian day 120), 10 days prior to extrusion (Fig. 9). The magma migration-extrusion phase (from rapid increase in tilt and beginning of migration of mean hypocenter depth to extrusion) showed up as a well-defined peak in the RSAM plot (Fig. 10) separated from the surface phase of the eruption by a relatively quiet period of 24 h. The surface phase was characterized by continuous rockfall-avalanche activity associated with the growing lobe and a decrease in size and number of earthquakes. Another characteristic of the surface phase was a swift decrease in RSAM amplitude when the lobe stopped growing rapidly on 10 May (Julian day 130). The 2–3 day duration for both the migration-extrusion phase and the surface phase contrasts with the more than 10 days of seismic activity associated with the May 1985 eruption.

Tilt data. By May 1986, RSAM hardware had been wired for eight seismic stations located around Mount St. Helens. Tiltmeters were operating near Sauna on the crater floor north of the dome (SAUN), and at tilt site RUBY on the north flank of the dome (Fig. 2). The progress of the changes in seismicity and tilt (coseismic deformation) were easily tracked by repeated plotting. A plot of RSAM data for seismic station YEL and SAUN radial tilt from the SAUN tiltmeter site showed coinci-

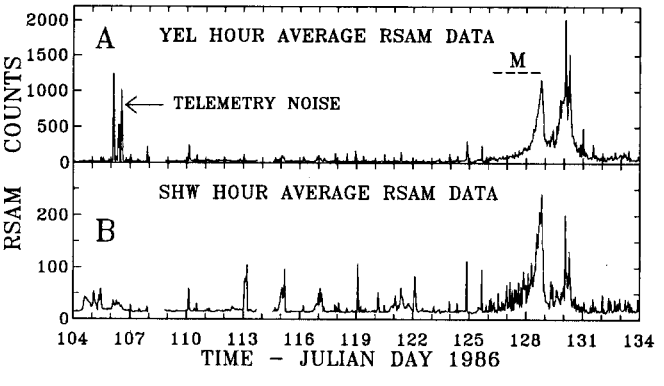

Fig. 9 A–B. RSAM plots of hourly average data for stations YEL and SHW from 14 April (Julian day 104) to 14 May (Julian day 134), 1986. The magma migration phase of the May eruption is the interval indicated by *M* and the surface phase of the eruption was associated with the RSAM peak after the interval indicated by *M*. Spikes on the left side of the YEL plot were associated with telemetry noise on the YEL radio link

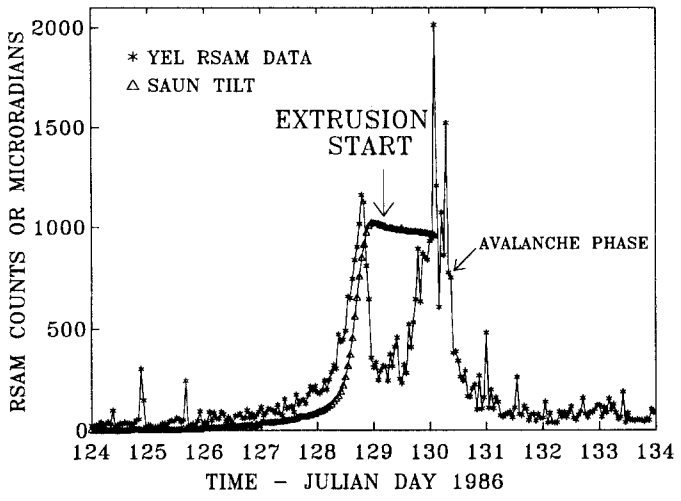

Fig. 10. May 1986 plot of hourly average RSAM digital counts for station YEL and radial tilt for SAUN tiltmeter station on a common time scale. RSAM for station YEL peaked at 1900 UT 8 May (Julian day 128), 1986. Tilt for SAUN tiltmeter station reversed direction, or south down several hours later. The extrusion of lava was assumed to have taken place at this time. The SAUN tiltmeter installation was destroyed during the peak of the avalanche phase

dent exponential increases in data values (Fig. 10). There was rapid increase in outward tilt at tilt site RUBY at the same time as tilt site SAUN, but RUBY went off scale (readings exceeded 10 000 microradians) at 1400 UT 8 May (Julian day 128). Photographic evidence during the October 1986 eruption indicates that extrusion began 12 h after the peak in RSAM data, at the beginning of slow inward tilt at the SAUN tilt site. The SAUN tilt site was destroyed at 0240 UT on 9 May (Julian day 129) by an avalanche from the new lobe. Slow inward tilt during the second increase in RSAM data supported the conclusion that seismicity following the initial peak was related to rockfalls and avalanches associated with the breakup of the dome and extrusion of the new lobe. A net outward tilt of about 500 microradians was recorded at the SAUN tilt site.

The October 1986 eruptive episode

Narrative. The late October 1986 eruptive episode resulted in a lava lobe slightly smaller in areal extent than the May 1986 lobe. Preliminary volume estimates for the October episode are about 9×10^6 m^3. That estimate takes into account lateral displacement of parts of the dome to accommodate new magma, particularly the September 1984 lobe, which was intensely disrupted. The initial peak in seismicity occurred at 0000 UT on 22 October (Julian day 295), and by 1200–1300 UT, timed photography of the dome showed that extrusion had begun. There was no rockfall-avalanche phase like that during the May 1986 episode, probably because the extrusion was inherently more stable during the October episode. The development of tear and thrust faults on the crater floor and talus slopes on the west and southwest sides of the dome, more or less along the extension of the May 1985 graben, were notable features of the episode (Swanson and Holcomb 1989).

RSAM data. The first indication of an impending eruptive episode was a sequence of earthquakes that began on 13 September (Julian day 256), 1986. While station YEL showed a count of about 20 earthquakes that day, the dome seismic station (DIO) recorded 750–1000 small magnitude earthquakes. Within 5 days, activity was back down to a few earthquakes per day. Less intense but otherwise similar sequences occurred on 22 September (Julian day 265), 30 September (Julian day 273), and 5 October (Julian day 278). One unconfirmed explosion event occurred on 9 September (Julian day 252). After 9 October (Julian day 282), earthquake counts at station YEL remained above 10 per day and increased to over 100 per day by 20 October (Julian day 293), less than 2 days before extrusion began.

RSAM plots (Fig. 11) of seismic activity in September–October 1986 were not as distinctive as those for April–May 1986, due to less-than-ideal conditions within the crater: avalanches and rockfalls from the crater walls resulted in a more complex seismic record. However, the plots (Fig. 12) did show the characteristic buildup in average amplitude during the last 2–3 days prior to extrusion. The first peak in RSAM data was followed by a second peak at 0600 UT. We can only speculate that the saddle in the station GDN RSAM plot is related to the change in seismicity accompanying the transition from crater floor to dome deformation. We also speculate that the second increase in average amplitudes was a result of earthquakes associated with intrusion of magma into the dome and subsequent thrust faulting beneath the west side of the lava dome. RSAM data for station GDN initially peaked shortly after 0000 UT on 22 October (Julian day 295). Timed

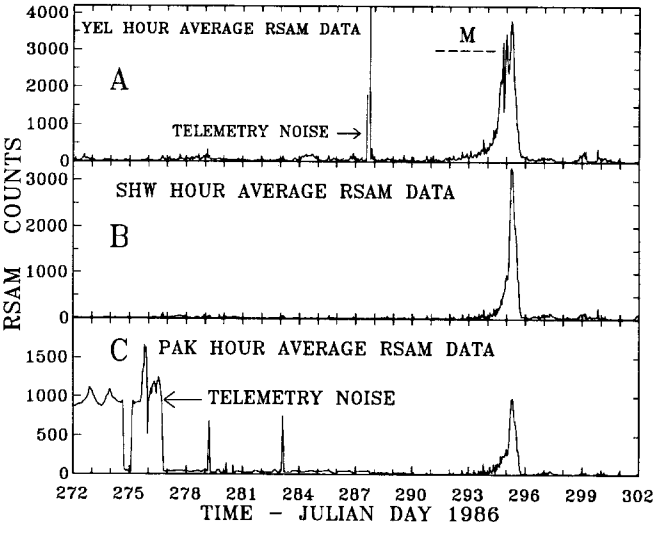

Fig. 11 A–C. RSAM plots of hourly average data for seismic stations *YEL*, *SHW*, and *PAK* from 29 September (Julian day 272) to 29 October (Julian day 302), 1986. The magma migration phase for the October eruption is indicated by the interval *M*

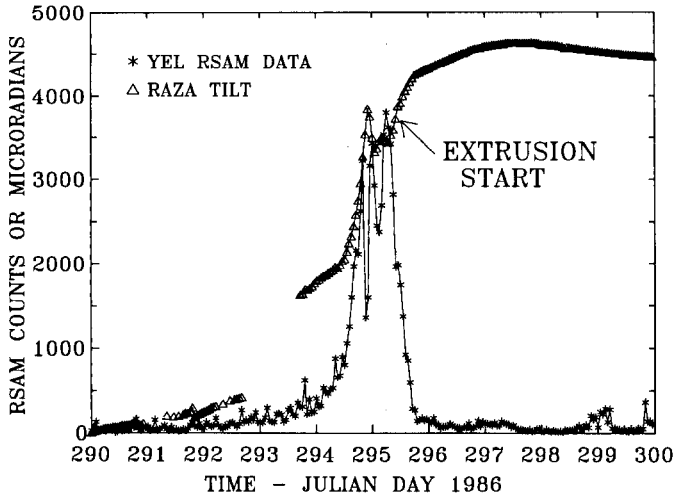

Fig. 12. September–October 1986 plot of RSAM digital counts for YEL seismic station and radial tilt for RAZA tiltmeter station on the same time axis

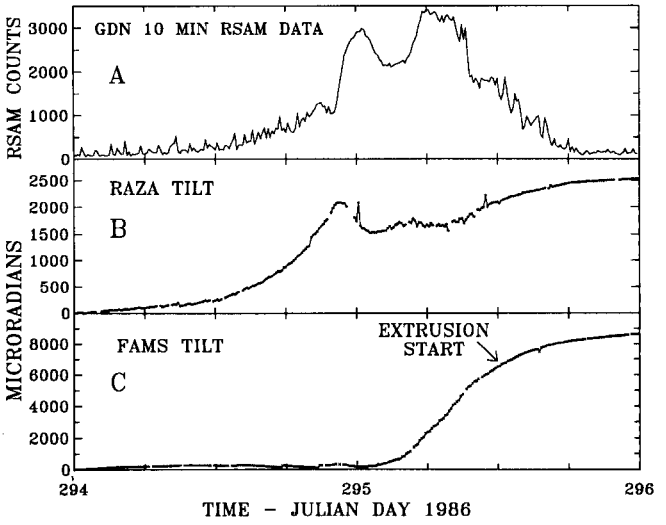

Fig. 13. **A** Plot of hourly average GND RSAM data for two days beginning at 0000 UT 21 October (Julian day 294), 1986. **B** Plot of tilt for station RAZA the same time window as Fig. 11a. **C** Plot of FAMS tilt for the same time window as Fig. 11A and B

photographs showed that extrusion in the summit area of the dome began between 1200 and 1300 UT.

Tilt data. All four tilt stations (FAMS, OOPS, RAZA and SWLP, Fig. 2) operating on the dome during October 1986 showed rapid increases in outward tilt that corresponded to the rapid increase in RSAM data at all seismic stations. In addition, the October 1986 RSAM and tilt data provided evidence for different tilt responses, depending on the location of the tiltmeter site relative to the center of deformation and whether or not the site was located on the dome or the crater floor. Two tilt stations (RAZA and SWLP) showed significant outward tilt (inflation of about 200 microradians per day) beginning 7–8 days prior to extrusion. More rapid inflation (5000 to 10000 microradians per day) began 48–72 h prior to extrusion. The inclinometer at the SWLP tilt site recorded more than 10° of tilt in the last 24 h before it was destroyed. Rapid inflation starting 18–20 h later was recorded at tilt stations OOPS and FAMS. Tilt data from the RAZA tilt site have been plotted with RSAM data from seismic station YEL (Fig. 12) to show that tilt was coseismic, as in previously described eruptive episodes. RSAM data peaked at 0600 UT 22 October (Julian day 295), 1986. Timed photography confirmed extrusion between 1200 and 1300 UT.

The first peak in RSAM data and a corresponding decrease in outward tilt on the crater floor represent the breakthrough of magma into the dome and the relaxation of stress between the magma and conduit walls near the crater floor-dome base interface (Fig. 13). The second phase of dome tilt observed at three tilt stations, and the corresponding drop in seismicity, were very likely associated with the intrusion of magma into the dome and thrust faulting beneath the west side of the dome. The 2-day duration of the magma migration-extrusion phase was similar to that of the May 1986 eruptive episode. The October 1986 eruptive episode was not accompanied by an extended surface phase like that of May 1986.

RSAM data for two explosion events at Mount St. Helens

31 December 1985

The first explosion (gas/ash emission) event recorded on the RSAM system occurred on 31 December 1985, at 0000 UT. About 100 high-amplitude, short-coda-length events (<35 s) were recorded by the seismographs for seismic stations NSP and GDN between 0000 UT and 0145 UT. Of these, only the largest events (shown in Fig. 14) were visible on the analog seismogram for station SHW (4 km to the SW). The largest event, 30 mm peak-to-peak on the CVO helicorder record, was assigned a preliminary coda magnitude of 1.5 by the University of Washington. The earthquakes were accompanied by a 2–3 times increase in the background noise level (Fig. 15) of the dome seismic station NSP from 0041 to 0200 UT. The high-frequency (peak uncorrected spectra near 12–13 Hz) tremor-like signal became strong enough to be recorded at the seismic station GDN at 0108 UT. The high-frequency tremor-like signal was assumed to be fumarolic noise generated by degassing through a vent located a few hundred meters south of station NSP. Dominant frequencies occurred above 10 Hz in contrast to typical harmonic tremor which is commonly dominated by frequencies below 4 Hz. The high-frequency noise is very similar to geyser noise studied by Kieffer (1984).

The three largest earthquakes were recorded by RSAM as spikes well above the background noise level

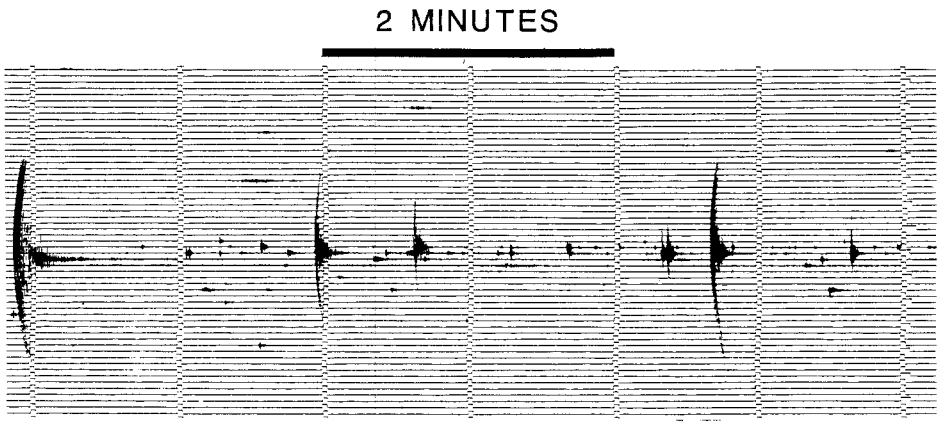

Fig. 14. A 6.5-min wide section of the analog seismic record for GDN on 30–31 December 1985. The largest amplitude event (0108 UT on 31 December) had an estimated coda magnitude of 1.8. Translation rate for the seismic record is 15 min per line

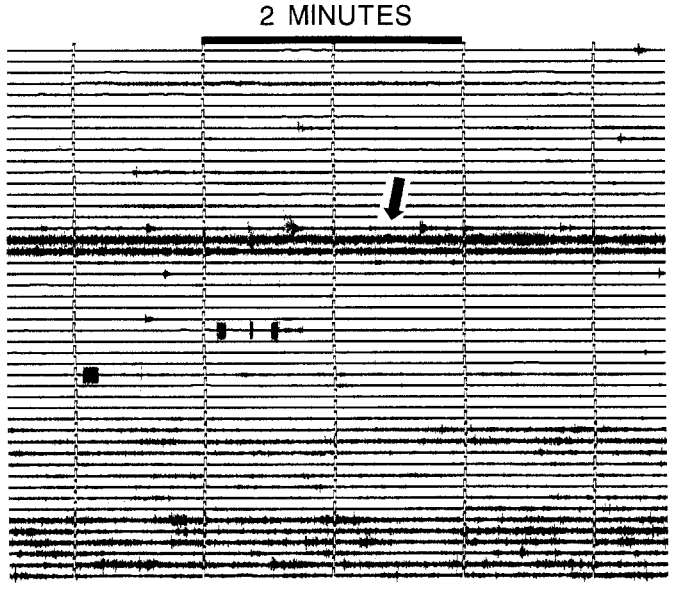

Fig. 15. A 5-min wide section of the NSP (first telemetry station installed on the dome) analog seismic record. Increase in high-frequency background noise level is indicated by the *arrow*. The helicorder (or heat sensitive) record did not clearly reproduce earthquake signatures

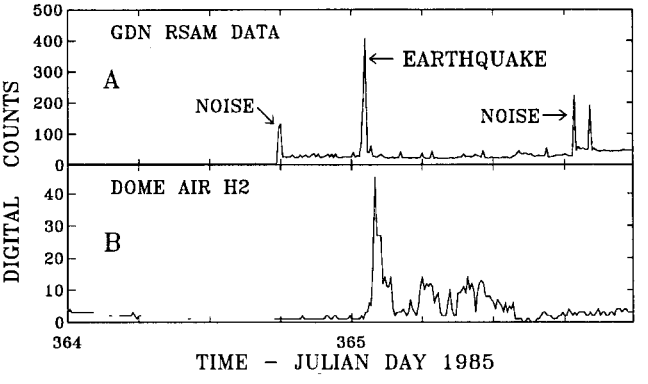

Fig. 16. A RSAM plot of the highest 1-min value in a 10-min interval for seismic station GDN from 30 to 31 December (Julian day 364 and 365), 1985. Spike to the left of the earthquake identified as noise is a result of connection of GDN seismic signal to the input of RSAM system. Two spikes to the right identified as noise were a result of wiring modification to RSAM system. **B** Plot of output from hydrogen sensor operating on the dome at the time of the explosion event of 31 December (Julian day 365), 1985. The hydrogen event occurred shortly after the magnitude 1.8 earthquake at 0108 UT

(Fig. 16a). RSAM data from station NSP was lost in December due to a poor electronic connection in the system. The smaller increase in background noise at station GDN can be identified by a small change in the base level of the station's RSAM plot. The sequence of earthquakes and accompanying high-frequency tremor-like signals at stations NSP and GDN suggested a small explosion (gas/ash emission as a result of a phreatic or phreatomagmatic explosion) similar to many others which had been observed earlier. Telemetered data from a volcanic gas sensor on the dome confirmed the increased emission of gas. The gas data (Fig. 16b) peaked about 1 h after the onset of earthquake activity.

April 1986

The next recorded sequence of explosion events occurred during the month preceding the eruptive episode of 9 May 1987. About 50 possible explosion events were identified from the RSAM data. Confirmation of each was not possible due to failure of telemetry from the gas sensor, but field observations of ash over fresh snow confirmed the larger events. Ideal crater conditions, low snow fall, freezing temperatures, and low wind noise resulted in relatively low background noise level at most seismic stations. As in late December 1985, individual earthquakes accompanying explosion activity showed as spikes on RSAM plots (Fig. 17a and b), and lower level high frequency noise showed as slightly elevated base levels. At 0115 UT on 17 April (Julian day 107), NSP seismic station was disabled by ballistic debris (Fig. 17a) from a relatively large explosion event. There were no significant changes in tilt associated with any of the explosion events in 1985 and 1986. It was not possible to clearly identify the explo-

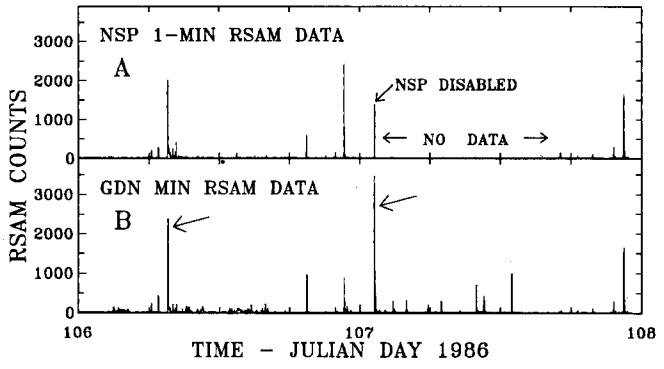

Fig. 17. A RSAM plot of seismic station NSP 1-min data from 16 April (Julian day 106) to 18 April (Julian day 108), 1986. Explosion debris associated with the event (at 0115–0120 UT on 17 April (Julian day 107) disabled the NSP seismic station. **B** RSAM plot of seismic station GDN 1-min data from 16 April to 18 April 1987. The largest events assumed to be associated with explosion events are indicated by *arrows*

sion events in December 1985 and spring of 1986 as phreatic or phreatomagmatic explosions.

Conclusions

The CVO RSAM system has been in operation since the spring of 1985. From 1985 to 1986 there were three dome-building eruptive episodes at Mount St. Helens; from each episode we have learned how to better interpret RSAM plots together with seismic and other tilt data. During all three episodes, similar rapid increases in seismicity began less than 48 h prior to the peak in RSAM data. Large changes in tilt, indicating inflation and the upward movement of magma, accompanied rapid increases in RSAM data. Clearly, RSAM data can be used for the prediction of dome-building eruptions at Mount St. Helens. The shape of RSAM plots following the initial peak in seismicity appears to depend on the volume of magma involved and events related to the intrusion of magma into the dome and its subsequent extrusion. Thrust faulting on the crater floor associated with lateral displacement of the crater floor and dome resulted in extended periods of seismicity during the May 1985 and October 1986 episodes. Instabilities accompanying the disruption of the dome by intruded magma-generated rockfalls and avalanches produced large-amplitude signals on seismic stations within the crater. Similarly, mass movement of newly extruded magma over the sides of the dome also generated rockfall/avalanche signals on crater seismometers.

Our experience at Mount St. Helens has shown that RSAM data cannot be used to predict phreatic or phreatomagmatic explosions. We also recognize the limitations of RSAM data during late-spring and summer crater conditions, when rockfall and avalanche conditions are optimum within the crater at Mount St. Helens. Melting snow in late spring and dry conditions during the summer promote rockfalls and avalanches from the crater wall. Telemetry failures also introduced problems in interpretation. Ambiguity in interpretation can be eliminated by comparison of RSAM data with other real-time data, such as tilt, gas, displacement, and various meteorological information. Visual examination of seismographs usually eliminates possible misinterpretation.

RSAM is an easy-to-implement and convenient-to-use method of tracking the intensity of seismic activity associated with volcanic eruptions in near real time. The value of RSAM data is best demonstrated by a recent application of an RSAM system in the monitoring of Redoubt volcano (Alaska Volcano Observatory Staff 1990). In addition to using RSAM data for predicting a number of major eruptions, RSAM data played a crucial role in the decision to evacuate the Drift River Oil Terminal hours before a major explosive eruption on 2 January 1990.

Acknowledgements. The authors credit Dr. R. Schick for the origin of the idea of looking at the amplitude envelope of a seismic signal to document the time history of seismicity associated with volcanic eruptions. We thank L. Topinka for her effort in obtaining photographic evidence for the time of extrusion for the October 1986 dome-building episode. We also gratefully acknowledge the early technical reviews by D. W. Swanson, P. Okubo, D. Dzurisin. Journal reviews by P. W. Lipman, S. D. Malone, and S. R. McNutt significantly improved the paper. G. Varanas and P. Johnson provided additional helpful comments.

References

Aki K, Richards PG (1980) Quantitative seismology, theory and methods. WH Freeman, San Francisco, Calif, 932 p

Alaska Volcano Observatory Staff (1990) The 1989–1990 Eruption of Redoubt volcano. EOS:71:265272–273275

Decker RW (1973) State-of-the-art in volcano forecasting. Bull Volcanol 37:372–393

Decker RW (1986) Forecasting volcanic eruptions. Ann Rev Earth Planet Sci 14:267–291

Endo ET, Dzurisin D, Murray T, Syverson K (1987) The rate of magma ascent during dome building at Mount St Helens (abstract). Abstract volume Hawaii Symposium on How Volcanoes Work, Hilo, Hawaii, p 64

Gutenberg B, Richter CF (1956) Magnitude and energy of earthquakes. Estratto da Annali di Geofisica 9:1–15

Hurst AW (1985) A volcanic tremor monitoring system. J Volcanol Geotherm Res 26:181–187

Kieffer SW (1984) Seismicity at Old Faithful Geyser: an isolated source of geothermal noise and possible analogue of volcanic seismicity. J Volcanol Geotherm Res 22:59–95

Korneff T (1966) Introduction to electronics. Academic Press, NY, 545 p

Koyanagi RY, Meagher K, Klein FW, Okamura AT (1975) Hawaiian Volcano Observatory Summary 75, 117 p

Lee WHK, Stewart SW (1981) Principles and applications of microearthquake networks. In: Advances in Geophysics, Supplement 2. Academic Press, NY, 293 p

Malone SD, Boyko C, Weaver CS (1983) Seismic precursors to the Mount St Helens eruptions in 1981 and 1982. Science 221:1376–1378

Minakami T (1960) Fundamental research for predicting volcanic eruptions, pt. 1. Bull Earthquake Res Inst 38:497–544

Minakami T (1974) Prediction of volcanic eruptions. In: Civetta L, Gasparini P, Luongo G, Rapolla A (eds) Physical volcanology. Amsterdam, Elsevier, pp 313–333

Minakami T, Hiraga S, Miyazaki T, Uchibori S (1969) Fundamental research for predicting volcanic eruptions, pt. 2. Bull Earthquake Res Inst 47:893–949

Murray TL, Endo ET (1986) BOB, a computer graphics tool for real-time integrated volcano monitoring. EOS 67:397

Nakamura Y (1977) Detection and analysis of acoustic emission signal. In: HR Hardy Jr, FW Leighton (eds) Proceedings First Conference on Acoustic Emission/Microseismic Activity in Geologic Structures and Materials 2:445–457

Nishi K (1987) Automatic data processing system for volcanic earthquakes and tremors, Annuals Disaster Prevention Res. Inst Kyoto Univ 30B-1:1–18

Norwack R, Aki K (1984) The two-dimensional gaussian beam synthetic method:testing and application. J Geophysical Res 89:7797–7819

Richter CF (1958) Elementary Seismology. WH Freeman and Company, San Francisco, 768 p

Sassa K (1936) Micro-Seismometric study on eruptions of the Volcano Aso (Part II of the Geophysical studies on the Volcano Aso). Memoirs of the College of Science, Kyoto Imperial University, vol XIX, 1:11–56

Scandone R, Malone SD (1985) Magma supply, magma discharge and readjustment of the feeding system of Mount St Helens during 1980. J Volcanol Geotherm Res 23:239–262

Schick R (1988) Volcanic tremor-source mechanisms and correlation with eruptive activity. Natural Hazards 1:125–144

Schick R, Lombardo G, Patane G (1982) Volcanic tremors and shocks associated with eruptions at Etna (Sicily), September 1980. J Volcanol Geotherm Res 14:261–79

Swanson DA, Holcomb RT (1989) Regularities in growth of the Mount St Helens dacite dome, 1980–1986. In: Fink J (ed) Lava flows and domes. Springer, Berlin Heidelberg New York 24 p

Swanson DA, Casadevall TJ, Dzurisin D, Holcomb RT, Newhall CG, Malone SD, Weaver CS (1985) Forecasts and predictions of eruptive activity at Mount St Helens, USA: 1975–1984. J Geodynamics 3:397–423

Editorial responsibility: P. W. Lipman